

## Whole Body diffusion-weighted MRI: Normal lymph node distribution, volume and apparent diffusion coefficient (ADC) in healthy volunteers

Raphael Shih Zhu Yiin<sup>1</sup>, Giuliano Scattoli<sup>1</sup>, Dow-Mu Koh<sup>1</sup>, David J Collins<sup>2</sup>, Martin O Leach<sup>2</sup>, and Matthew D Blackledge<sup>2</sup>

<sup>1</sup>Department of Radiology, The Royal Marsden Hospital, Sutton, Surrey, United Kingdom, <sup>2</sup>CR-UK and EPSRC Cancer Imaging Centre, Sutton, Surrey, United Kingdom

**PURPOSE:** Whole body diffusion weight imaging (WB-DWI) is being used to evaluate nodal disease in lymphoma and metastatic nodal disease [1]. However, there is an overlap in the MR diffusion properties of malignant and non-malignant lymph nodes. An improved understanding of the DWI characteristics of normal lymph nodes would inform disease assessment. Hence, the aim of this study is to determine the distribution, volume and ADC values of normal lymph nodes throughout the body in normal individuals.

**MATERIALS AND METHODS:** Approval for this study was obtained from the local institutional research and ethics committees. 20 healthy adult volunteers without history of illness in the preceding 4 weeks were recruited and WB-DWI was performed to map the lymph nodes. **Imaging protocol:** WB-DWI images were acquired on a 1.5T MRI scanner (MAGNETOM Avanto, Siemens AG, Healthcare Sector, Erlangen, Germany) using the following imaging parameters: Matrix = 150x144, Partial Fourier = 6/8, TE = 64.8ms, TR = 14.6s, Readout Bandwidth = 1961 Hz/px, b-values = 50 and 900s/mm<sup>2</sup>, trace weighted diffusion encoding, STIR fat suppression (TI = 180ms), Slice Thickness = 5mm, Field of View = 400x390 mm<sup>2</sup>. GRAPPA was applied to reduce distortion along the phase-encoding direction (R = 2). Images were acquired using 4 consecutive imaging stations comprising of 50 slices each to cover the top of the head to the level of the mid-thigh. **Image interpretation:** The b900 images were reviewed by two experienced radiologists on an OsiriX workstation and the nodes outlined with volumes of interest (VOI), using a semi-automated segmentation software (ICR, UK). For each lymph node and nodal site, the nodal volume and the median ADC values were recorded. Voxelwise ADC values of all lymph nodes were also obtained to derive the global ADC histogram of all the volunteers. The median ADC values were compared between nodal regions using a Mann-Whitney test, with a p-value of <0.05 taken as being statistically significant.

**RESULTS:** 7 women and 13 men were recruited, with a mean age of 34.8 years (range 22-60). 1028 nodes were identified and segmented. Nodal distribution on WBDWI was observed as follows: occipital (4%), cervical (33%), axillary (19%), intrathoracic (0.9%), mesenteric (1.2%), portal (1.1%), retroperitoneal (9%), pelvic (6%), inguinal (25%) and subcutaneous (0.8%). The mean nodal volume was 0.39 ml (range 0.09 – 3.4). The mean and median ADC voxel values of all lymph nodes by histogram analysis were 1.13 and 1.12 ± 0.27 (10<sup>-3</sup> mm<sup>2</sup>/s) respectively. The other ADC parameters are as follows: the mean ADC skewness in individual nodes was 0.25 ± 0.02; and the mean ADC kurtosis was 0.34 ± 0.04. No gender nodal difference was observed. The intrathoracic, portal and retroperitoneal nodes showed significantly higher median ADC when compared with other nodal sites (p<0.05). Figure 1. shows the WB-DWI 3D MIP of the nodal distribution. Figure 2. shows the histogram analysis of median ADC values of the normal lymph nodes. Figure 3. shows the Box and Whiskers plot of median ADC values of various nodal regions.



Figure 1.

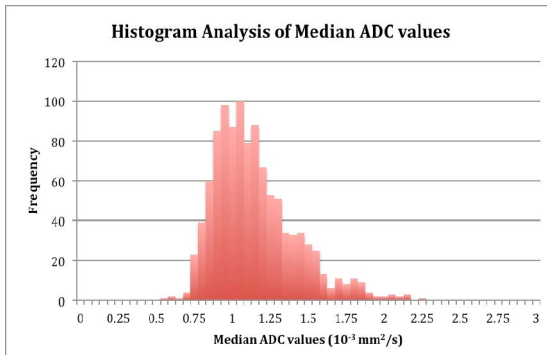


Figure 2. Population distribution of nodal median ADC values

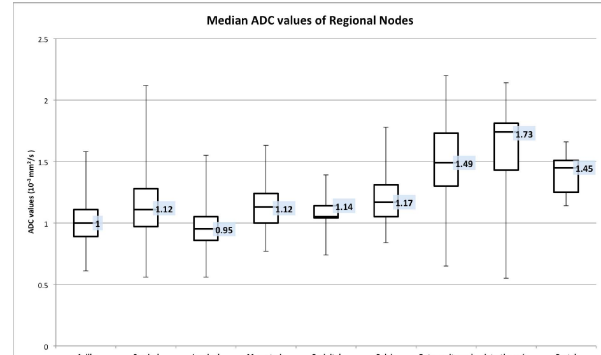


Figure 3. Numbers indicate Median values

**DISCUSSION:** Multiple studies have established the range of ADC values in metastatic adenopathy and lymphoma. However, data on ADC values of normal lymph nodes is lacking in the context of a healthy population. Most of the current literature on ADC values of normal/benign lymph nodes was measured in patients with pre-existing malignancy. Nonetheless, Kwee et al showed mean ADC values of normal lymph nodes in the range of 1 to 1.18 (10<sup>-3</sup> mm<sup>2</sup>/s) in two separate studies [2,3], consisting of 16 and 20 healthy volunteers respectively, which are similar to the mean ADC value (1.13) observed in our study. However, only cervical, axillary and inguinal lymph nodes were measured as according to the authors' experience, normal lymph nodes in the chest and abdomen regions are usually not depicted at DWI and hence not scanned in the studies. Our results show the majority of normal lymph nodes observed on WB-DWI are distributed in the cervical, inguinal, axillary, retroperitoneal and occipital regions (order of decreasing frequency). The detection of normal lymph nodes in the thorax and mesentery is low, which supports Kwee et al experience, but retroperitoneal nodes contribute to 9% of total body nodes. Higher mean and larger range of ADC values for intrathoracic and portal nodes could be attributed to sampling bias due to the small numbers measured. However, higher ADC values in the retroperitoneal region may be related to motion. As is now known the ADC varies over the field of view due to gradient non-linearity [4]; this may also contribute to variation in ADC estimates at different nodal sites. In our study, we also defined the full ADC histogram characteristics of normal lymph nodes, which may inform future disease assessment when compared with diseased states.

**CONCLUSION:** The majority of the nodes are distributed in the cervical, inguinal, axillary, retroperitoneal and occipital regions (order of decreasing frequency). Higher ADC values in retroperitoneal nodes may be due to motion, while the higher mean and larger range of ADC values for intrathoracic and portal nodes could be attributed to sampling bias. The ADC histogram characteristics of normal lymph nodes may inform the assessment of nodal disease.

**REFERENCES:** [1] Mao et al. Curr Radiol Rep (2014) 2:36 [2] TC Kwee et al. Magn Reson Mater Phy (2011) 24:1 – 8. [3] TC Kwee et al. European Journal of Radiology 75 (2010) 215 – 220. [4] DI Malyarenko et al. Mag Reson Med (2013).

Acknowledgements: CRUK and EPSRC Cancer Imaging Centre in association with the MRC and Department of Health grant C1060/A10334; NHS funding to the NIHR Biomedical Research Centre and post-doctoral fellowship funding by the NIHR (NHR011X); An Experimental Cancer Medicine Centre Network award (C51/A7401 & C12540/A15573); MOL is a NIHR Senior Investigator.